Food Hydrocolloids 102 (2020) 105607

Contents lists available at ScienceDirect

Food Hydrocolloids

journal homepage: http://www.elsevier.com/locate/foodhyd

Time-dependent self-association of spruce galactoglucomannans depends on pH and mechanical shearing

Mamata Bhattarai [a,*], Fabio Valoppi [a,b], Sami-Pekka Hirvonen [c], Sami Hietala [c], Petri Kilpeläinen [d], Vladimir Aseyev [c], Kirsi S. Mikkonen [a,b]

[a] Department of Food and Nutrition, Faculty of Agriculture and Forestry, P.O. Box 66, University of Helsinki, Finland
[b] Helsinki Institute of Sustainability Science (HELSUS), Faculty of Agriculture and Forestry, University of Helsinki, Finland
[c] Department of Chemistry, Faculty of Science, P.O. Box 55, University of Helsinki, Finland
[d] Natural Resource Institute Finland, Tietotie 2, 02150, Espoo, Finland

ARTICLE INFO

Keywords:
Hemicelluloses
Spruce galactoglucomannans
Self-association
Hydrocolloids

ABSTRACT

The demand for naturally derived, functional and cost-effective raw materials for various food applications is escalating. Spruce wood is a sustainable and abundant, but underutilized source of novel hydrocolloids—galactoglucomannans (GGM). Pressurized-hot water extracted GGM with an intermediate molar mass are hypothesized to form colloidal solutions. To design superior quality products from GGM, an understanding of their colloidal stability and their potential effect in multiphasic systems is required. The present study addresses the functionality of GGM by characterizing their properties in a bi-phasic system, and for the first time, their time-dependent colloidal stability at different extrinsic conditions— pH, ionic strength and after the application of high-intensity mechanical shearing. Amongst the conditions studied, the colloidal stability of aqueous GGM solution was highly pH dependent. The results showed that an intermediate molar mass polysaccharide like GGM formed inter-/intra molecular assemblies, which grew over time, depending on the composition and processing of the aqueous medium. The molecular dispersion of GGM and their dynamic behavior was also compared to solutions of known food hydrocolloids—gum Arabic and hydroxypropylmethyl cellulose. The observed solution properties explain the hydrocolloid functionality of GGM and contribute to design of colloidal polysaccharide systems in food application.

1. Introduction

A colloidal system is referred to as biphasic system having characteristics between that of a true solution and suspension. There is no collective consensus on size scale of a colloid, which is often described as “the world of neglected dimensions”. Literature suggest the size of colloid from 1 nm up to 1 μm (Tadros, 2017). Hydrocolloids, as the name suggests, have hydrophilic colloidal particles and they are widely utilized to design complex multiphasic food systems that are able to control microstructure, improve shelf-life, or deliver bioactive compounds, for example (Dickinson, 2003). Food hydrocolloids include proteins, as well as native and modified polysaccharides from plants, animals and microbes. Polysaccharides represent the major category of food hydrocolloids. Most common plant-based food hydrocolloids are native high molar mass polysaccharides like gum Arabic, pectin, guar gum and konjac gum, as well as modified polysaccharides such as derivatives of cellulose and starch (Dickinson, 2003). The ability of polysaccharides to modify the surface/interfacial activity and form viscous solutions and gels is utilized in the development and stabilization of multiphasic systems (Dickinson, 2003). Hence, from an application point of view, their solubility in an aqueous medium is an important consideration.

As much as polysaccharides are complex, their solubility is an equally complex phenomenon. Solubility relates to the balance between polymer-solvent and polymer-polymer interaction, which is reached in so called “theta” solvent (Guo, Hu, Wang, & Ai, 2017). The polymer-polymer interaction can be inter- or intramolecular in the form of physical entanglements, hydrogen bonding or hydrophobic interaction. These are intrinsic to polysaccharides’ properties such as, degree of polymerization and branching, carbohydrate composition and non-polysaccharide residues (Whistler, 1973). These intrinsic characteristics are influenced by the solution conditions, for e.g. pH, ionic strength and temperature. Inter-/and intramolecular association occur

* Corresponding author.
E-mail address: mamata.bhattarai@helsinki.fi (M. Bhattarai).

https://doi.org/10.1016/j.foodhyd.2019.105607
Received 29 September 2019; Received in revised form 13 December 2019; Accepted 17 December 2019
Available online 23 December 2019

in almost all polysaccharides, including: gum Arabic (GA) (Sanchez et al., 2018); pectin (Fishman, Cooke, Hotchkiss, & Damert, 1993; Walter & Matias, 1991); galactomannans (guar, locust bean gum) (Gittings et al., 2000); konjac glucomannans (konjac gum) (Ratcliffe, Williams, Viebke, & Meadows, 2005); and cellulose derivatives, like methylcellulose and hydroxypropylmethyl cellulose (HPMC) (Bodvik et al., 2010). These associations create colloidal features; discrete structural entities, such as aggregates or continuous networks like gels.

Emulsions, a common example of multiphasic system in food products, are significantly influenced by the solubility of polysaccharides that are used to create and stabilize them. At the emulsion interface, on one hand, the intra-/inter molecular association of adsorbed polysaccharides adversely affects sterically stabilized system resulting flocculation and eventually emulsion instability via coalescence (Dickinson, 2003; Tadros, 2017). On the other hand, polysaccharide-based particles formed as a result of their partial insolubility are known to stabilize interface or near-interface, widely discussed as Pickering stabilization (Dickinson, 2017). Similarly in the continuous phase of emulsions, unadsorbed polymers at a high concentration are known to induce depletion stabilization (Kim, Hyun, Moon, Clasen, & Ahn, 2015; Semenov & Shvets, 2015). However, to the best of our knowledge, it has not been discussed in relation to natural polymers.

Biopolymer-based functional colloids are on high demand as they address the growing need of functional nano-and microstructures in food applications (Dickinson, 2017) from a technological point of view and at the same time, address consumers' concerns about the origin and sustainability of their consumption. In the framework of a circular economy and integrated bio-refinery concept, the application of wood hemicelluloses has garnered interest (Employment, 2017), due to their abundant availability and underutilization. Galactoglucomannans (GGM) are the main hemicelluloses present up to 25% in the industrially important softwood-variety, spruce, that is used for pulping, papermaking and timber (Sjöström, 1993; Willför, Sundberg, Tenkanen, & Holmbom, 2008). GGM is composed of partially acetylated β-(1 → 4) linked D-Man*p* and D-Glc*p* units substituted by α-(1 → 6) linked D-Gal*p* residues. On average, one acetyl unit substitutes per 3–4 hexose units at C-2 and C-3 position (Sjöström, 1993). Other softwood-originated hemicelluloses include arabinoglucuronoxylans (7–10%), arabinogalactan, and minor amounts of pectic polysaccharides such as galacturonans (Sjöström, 1993).

Pressurized hot water extraction process has been reported to yield GGM with novel hydrocolloid properties from forest by-products, such as sawdust and woodchips in a safe and environmentally friendly way (Kilpeläinen et al., 2014; Pitkänen, Heinonen, & Mikkonen, 2018), although other methods have been developed (Schoultz, 2015; Willför, Rehn, Sundberg, Sundberg, & Holmbom, 2003). GGM have shown promising application as emulsifiers and stabilizers in dispersed systems like oil-in-water (O/W) emulsions (Bhattarai et al., 2019; Mikkonen et al., 2019; Mikkonen, Merger, et al., 2016; Valoppi et al., 2019). Their protection ability against emulsion breakdown and lipid oxidation was reported to be even better than that of the "standard" polysaccharide hydrocolloid, GA, and its recent challenger, corn fiber gum (Bhattarai et al., 2019; Lehtonen et al., 2018; Mikkonen, Merger, et al., 2016). Thus, GGM are envisioned to compete against standard food hydrocolloids in terms of functionality, cost and availability in the future.

Our previous study indicated that adsorption of GGM at the droplet interface partially explained emulsion stability (Bhattarai et al., 2019). With the low surface activity of purified GGM (Mikkonen, Merger, et al., 2016), their ability to prevent droplet coalescence in emulsions was hypothesized to be due to a mixed effect of steric and Pickering-type stabilization arising from GGM assemblies (Bhattarai et al., 2019; Mikkonen, Merger, et al., 2016). The occurrence of assemblies have been previously reported in GGM obtained by Thermo-mechanical pulping (TMP) process and xylan obtained by acid hydrolysis (Kishani et al., 2019; Kishani, Vilaplana, Xu, Xu, & Wågberg, 2018; Westbye, Köhnke, Glasser, & Gatenholm, 2007). These samples had higher molar mass than Pressurized Hot Water Extracted GGM (PHWE GGM), with a reported molar mass of 10–12 kDa (Bhattarai et al., 2019; Mikkonen, Merger, et al., 2016). This molar mass of PHWE GGM is also on average 10^2–10^3 times lower than that of abundantly used hydrocolloids, like GA (Sanchez et al., 2018), pectin (Walter & Matias, 1991), galactomannans and glucomannans (Nishinari, Takemasa, Zhang, & Takahashi, 2007). However, considering the limitation of the conventional Size Exclusion Chromatography (SEC) that was used for molar mass analysis, where pre-filtration of samples is mandatory, we believe that information about larger structures in GGM has not been elucidated thus far. We speculate that structural entities are present in aqueous GGM solution. When unadsorbed GGM is present in the continuous phase of emulsions, such entities could influence the emulsion stability. Potential time-dependent self-association of GGM assemblies could thus affect the stability of colloidal systems based on GGM.

We hypothesize that aqueous GGM solution is partially composed of solvated polysaccharide chains and partially of discrete structural entities formed of associated polysaccharides. The aim of this study is therefore to understand the aqueous solution behavior of GGM extracts. The present work first compares the nature of aqueous GGM with the most abundantly used polysaccharide-hydrocolloid, GA (E414), and HPMC (E464). Second, we study the role of some extrinsic conditions, namely, solution pH, ionic strength and the application of high-intensity mechanical shearing on the associative properties of GGM. Third, we study the time-dependent self-association of GGM in comparison with GA and HPMC and at above-mentioned extrinsic conditions. To the best of our knowledge, this is the first study that addresses time-dependent self-association of wood polysaccharides in a systematic way, and the results provide valuable insight into their development as novel, bio-based food hydrocolloids.

2. Experimental section

2.1. Materials and reagents

GGM were obtained from spruce sawdust by using the PHWE process (Kilpeläinen et al., 2014). The concentrated extract from the process was precipitated using ethanol (1/8 concentrate/ethanol v/v). The ethanol precipitation process has been described in details in our previous study (Bhattarai et al., 2019). According to the monosaccharide analysis using acid methanolysis followed by gas-chromatography, about 86 wt% of the ethanol precipitated GGM were carbohydrates, which was obtained after summing up the monosaccharide quantities and applying the correction factor to compensate for the condensation reaction. The monosaccharides were 54.5 ± 0.05% mannose, 15.01 ± 0.02% glucose, 14.66 ± 0.09% xylose, 10.38 ± 0.06% galactose, 3.02 ± 0.00% galacturonic acid and 2.41 ± 0.02% 4-O-methyl galacturonic acid (Bhattarai et al., 2019). The percentages are expressed on dry GGM. The reported values are mean and standard error of mean from our previous study (Bhattarai et al., 2019). Arabinose and rhamnose sugars were present in trace quantities (less than 1%) (Mikkonen et al., 2019) and below the quantification level in the study by Bhattarai et al. (2019). The estimated molar mass was ~12 kDa analyzed by SEC using pullulan standards (Bhattarai et al., 2019). The total phenolic content and extractives were measured as 15.8 mg Gallic acid equivalent/g and 0.36 mg/g GGM (Mikkonen et al., 2019). Based on these analyses, the material of study was GGM-rich extract, which contained minor amounts of other softwood hemicelluloses and naturally co-extracted phenolic compounds and extractives.

GA was kindly provided by Kerry Group (Tralee, County Kerry, Ireland). According to the manufacturer, the product was exudate from *Acacia senegal* which contained about 95% arabinogalactopeptide, in addition to minerals and trace elements. The molar mass of GA has been reported between 2.5 × 10^2 to 2.6 × 10^3 kDa (Sanchez et al., 2018). HPMC was purchased from Sigma-Aldrich (Saint Louis, MO, USA). The average number-based molar mass was ~10000 g/mol i.e. 10 kDa,

according to the manufacturer.

Citric acid monohydrate and hydrochloric acid was from VWR's BDH Chemicals (Belgium), disodium carbonate, sodium chloride, sodium hydroxide, and sodium azide was from Merck (Darmstadt, Germany).

2.2. Acetic acid calculation

To calculate the total content of acetyl groups in GGM, an alkaline treatment was performed to release the acetyl groups from GGM. A 5 mg/ml GGM was dissolved in 100 mM sodium hydroxide for approximately 24 h at room temperature (RT) (22 ± 1 °C) while stirring in magnetic stirrer at 120 rpm. The solution was neutralized by 1 M HCl. The released acetic acid content in the sample was measured using Acetic acid assay kit (K-ACET) (Megazyme, Ireland). The obtained acetyl groups % (w/w) was used to calculate degree of acetylation (DA) (Xu et al., 2010).

2.3. Sample preparation

GGM solutions were prepared in a two-component, sodium citrate-carbonate buffer: 25 mM sodium citrate-carbonate buffer at pH 3.6, 4.6, 7.2 and 10 were prepared by mixing citric acid monohydrate and disodium carbonate. The buffer components were calculated using Buffer Maker buffer calculator program (Borkowski, 2005) by keeping the amount of disodium carbonate constant. Citrate-carbonate buffer covered a wide range of pH values, keeping a low ionic strength of the buffer, which was between 50 and 80 mM. The ionic strength of the buffer was kept low to avoid interaction from ions of the buffer system with the GGM. This was important to understand the role of added ions on the behavior of GGM. The buffer capacity of the citrate-carbonate buffer is explained in the supplementary data (Fig. B1). All buffers were filtered at RT with a 0.2 μm filter prior to use in order to avoid dust contamination.

Aqueous solutions of GGM (2% w/v) were prepared by dissolving GGM in the buffers at all four studied pH values, for about 2 h in total, with magnetic stirring. To study the effect of ionic strength, 50 mM or 100 mM NaCl was added to GGM solutions at acidic pH (4.6) and alkaline pH (10) and mixed for a further 30 min. The pH of solutions was monitored on the preparation day and after two and four weeks of storage in a controlled temperature room at 23 ± 0.5 °C during the time-dependent study.

To study the effect of high-intensity mechanical shearing, the GGM solutions at pH 4.6 and pH 10 were mechanically mixed in an Ultra-turrax (T-18 basic, IKA, Staufen, Germany) for 2 min at 22000 rpm and passed through high-pressure homogenizer (Microfluidizer 110Y, Microfluidics, Westwood, MA, USA) configured with 75 μm Y-type F20Y and 200 μm Z-type H30Z chambers in a series, using 800–850 bar pressure and continuous process for 32 s—equivalent to 4 passes calculated with a flow rate of 460 ml/min and a total sample volume of 80 ml. The treatment was performed at RT.

Solutions of 0.5–2% w/v GA and HPMC was prepared in the same buffer system at pH 4.6 by dissolving them similarly to GGM, for 2–3 h at RT.

2.4. Sedimentation kinetics by Turbiscan

Turbiscan Stability Index (TSI) was used as a basis for evaluating sedimentation kinetics of the solutions. It is a simple and calibration free approach to study the destabilization kinetics—increase in TSI indicates changes on-going in the system. From the prepared solutions, 20 ml was poured into a semi-flat-bottom shaped glass vial to be measured by Turbiscan Lab expert (Formulaction, France). TSI was obtained from Turbisoft version 1.2 (Formulaction, France). The descriptions about the principle of Turbiscan and TSI are provided in the supplementary information.

The remaining solution was used for particle size measurement. Each GGM solution was divided into 3 ml aliquots in duplicate for particle size measurement during storage. Sodium azide at 0.02% (w/v) was added to the solutions to prevent microbial spoilage during storage. To compare the sedimentation kinetics of GGM with GA and HPMC at a comparable viscosity, 1% GGM, 1% GA and 0.5% HPMC solutions (all in w/v) were studied. This concentration of GA and HPMC was chosen based on viscosity measurement (presented further).

2.5. Viscosity measurement

To find the suitable concentration of GA and HPMC that would yield a similar viscosity to that of GGM, the viscosity of the aqueous solutions of GGM, GA and HPMC at 0.5, 1, 1.5 and 2% (w/v) was compared. Flow curves from the solutions were measured in triplicate with a DHR-2 rheometer (TA Instruments, USA) using a double gap cup geometry in strain-controlled mode ramping the shear rate from 10 to 600 s^{-1} at 22 °C.

2.6. Particle size and zeta potential measurement

The particle size distribution (PSD) and zeta potential of the samples was measured at 25 °C using a zetasizer (Zetasizer Nano ZS, Malvern Instruments), that uses 4 mW, 633 nm standard laser.

For PSD, a backscattering angle of 173° was used and two replicates were measured from each solution. Each replicate was measured in three runs. The previously prepared 1% GGM, 1% GA and 0.5 or 1% HPMC solutions were measured with 2x dilution, whereas 2% GGM solutions were 4x diluted. All dilutions were made in the same buffer used for sample preparation. The dilution was chosen during pre-trials to obtain an optimal concentration to avoid multiple scattering. In case of measurement of filtered samples, a 30 mm syringe Glass Micro Fiber (GMF) filter of pore size 0.7 μm (ThermoFischer Scientific, USA) was used. GMF filter material was chosen, as it has low interaction with other components of our samples based on our previous experience. For GGM solution, the measurement was performed on the preparation day, and after one, two and four weeks during storage. GA and HPMC solutions were measured only on the preparation day. Dispersion Technology Software (DTS Nano version 5.00, Malvern Instruments) was used for data collection and analysis. The intensity based PSD was obtained using Malvern's default general purpose algorithm, which was also used to calculate the mean particle size (in diameter) of polysaccharides in solutions.

The zeta potential of the aqueous GGM solutions was performed on the preparation day and after 4 weeks of storage. After loading the samples in the folded capillary cells and inserting into the instrument, they were equilibrated at 25 °C for 2 min. Next, three repeated measurements were obtained from at least 30 continuous readings on each sample. Smoluchowski equation was used for zeta potential calculation (Bhattacharjee, 2016). Samples were measured in duplicate when their zeta potential was low (close to zero).

2.7. Optical and Cryo-transmission electron microscopy

The GGM solutions were visualized using an Axiolab optical microscope (Carl Zeiss, Germany) equipped with Axiocam 305 camera or Axiocam MRc (Carl Zeiss, Germany).

For Cryo-transmission electron microscopy (Cryo-TEM), a 2% GGM solution was prepared at pH 4.6 as explained previously (section 2.2). The solutions before and after high-intensity mechanical shearing were vitrified by plunging into liquid ethane at −178 °C after 1 h of resting period at 22 °C. The vitrified samples were prepared from 3 μl aliquots with a Leica EMGP vitrification device on freshly glow-discharged Quantifoil R1.2/1.3 copper grids that were covered with holey carbon films. The samples were observed in a FEI Talos Arctica microscope operated at 200 kV. The images were recorded at a nominal magnification of 22,000× with a FEI Falcon 3 camera operated in a linear mode.

58 and 38 images were recorded from the untreated and treated samples, respectively.

2.8. Surface charge density and pKa determination

The surface charge density and pKa of GGM were measured by conductometric titration (Farris, Mora, Capretti, & Piergiovanni, 2012). A 0.5% (w/v) of GGM was dissolved in deionized water for 2 h at RT followed by degassing in an ultrasonic bath for 20 min. Initially, the pH of the solution was adjusted to 2.6 with 0.1 M HCl and 0.05 M NaOH was used to titrate afterwards. Conductivity was measured using a conductivity meter (CDM210, MeterlLab™, Radiometer Analytical, Cophenhagen) and pH was measured simultaneously. Measurements were performed in triplicate.

2.9. Statistical analysis

Independent samples *t*-test or one-way ANOVA followed by post-hoc Tukey's test was performed to differentiate the mean particle size of the GGM solutions obtained from the PSD measurement under different solution conditions using SPSS Statistics 25 (IBM Corp, USA). The mean particle size (n = 2 x 3) from each group was used to determine statistical significance at $p < 0.05$.

3. Results and discussion

3.1. Comparing the solution properties of GGM with known food hydrocolloids

For the characterization of GGM solution properties, our first approach was to understand the differences in the solubility of GGM with that of known food hydrocolloids, GA and HPMC by comparing their light transmittance in Turbiscan (Fig. 1A).

GGM was highly turbid with only about 63% of incident light being transmitted, compared to 83% and 88% being transmitted through GA and HPMC solutions, respectively. The transmission through the buffer at pH 4.6 (control) was about 88%, same as for HPMC. This indicates the presence of large/particulate entities in GGM solution compared to GA and HPMC.

In order to understand if GGM had large particulates in the solution, the particle size measurement of these hydrocolloid solutions was performed. From the autocorrelation function and intensity-based average particle size of three hydrocolloids (Fig. 1B), it was clear that GGM contained a high portion of large particles. This was also proven after a mild centrifugation (5000 g, 10 min); GGM solution had some sediment, while GA and HPMC had a negligible/absence of sediment (Fig. C1, supplementary data). In our recent study, we made a similar observation on the crude GGM process extract (prior to ethanol precipitation process). The sediment after a very high-speed centrifugation was identified as lignin (Valoppi et al., 2019). The trace content of phenolic compounds in GGM used in this study is expected to be in polymerized form as reported in recent studies (Lahtinen et al., 2019; Valoppi et al., 2019). The particle size of the supernatant was lower than reported in Fig. 1, however the reduction in particle size after centrifugation was the highest in GGM (data not shown), which indicated the existence of assemblies in GGM compared to GA and HPMC.

In our study, 1% GGM and GA exhibited similar solution behavior i.e., low viscosity at similar mass concentration in accordance to previous studies (Mikkonen, Merger, et al., 2016; Sanchez et al., 2018) and non-gelling ability. There are was no apparent shear thinning of GGM up until 2% GGM, which was the maximum studied concentration in this study. In an earlier study, PHWE GGM solutions had exhibited Newtonian behavior up to 30% (Mikkonen, Merger, et al., 2016). Previously, GGM obtained from TMP process have reported higher viscosity and shear-thinning behavior above 0.5% (Xu, Willför, Holmlund, & Holmbom, 2009). The observed rheological behavior was likely due to higher molar mass (39–46 kDa) of TMP GGM used in the study. Former studies have also reported higher molar mass of TMP GGM compared to PHWE GGM (Kishani et al., 2018; Mikkonen et al., 2019; Mikkonen, Xu, Berton-Carabin, & Schroën, 2016). This means that solution behavior of GGM will be highly dependent on the applied extraction method.

GA is a complex, highly branched polysaccharide composed of three fractions—arabinogalactan-peptide, arabinogalactan-protein complex and glycoproteins. Readers are advised to refer to Sanchez et al. (2018)

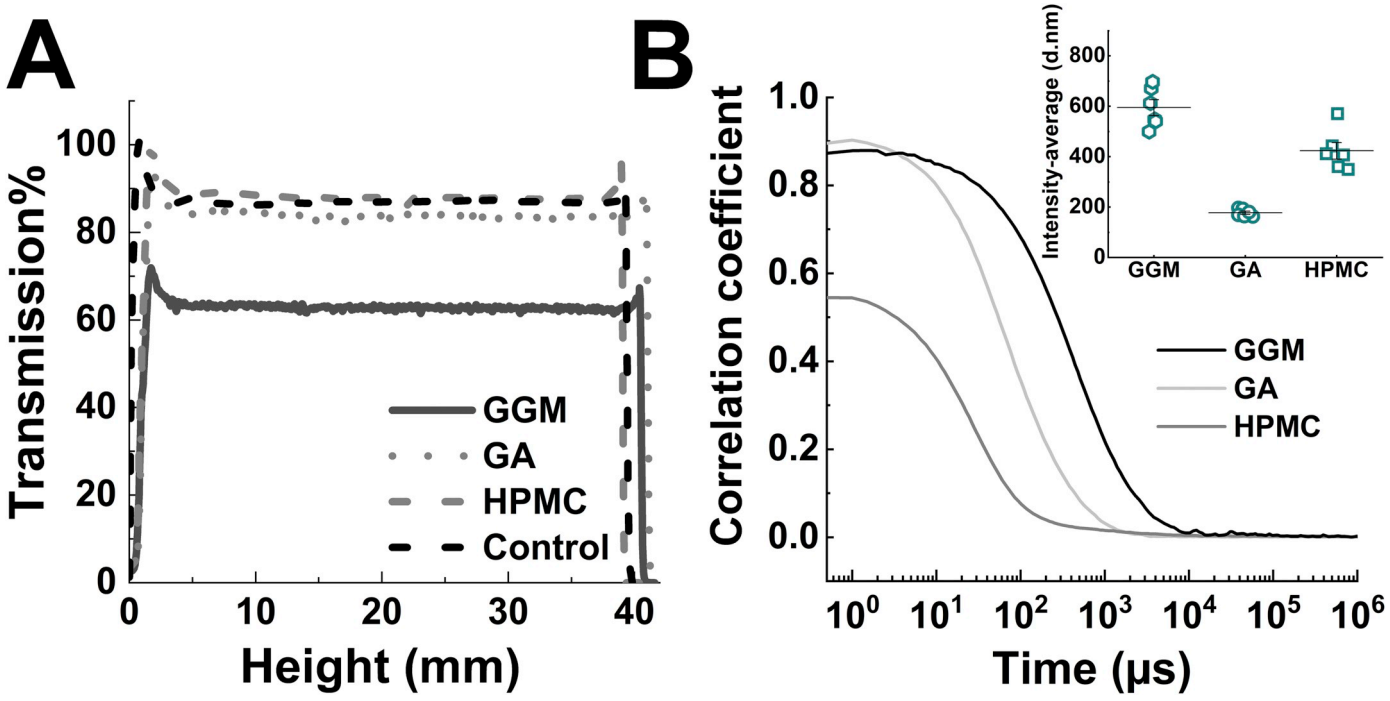

Fig. 1. (A) Transmission % of 1% galactoglucomannans (GGM), gum Arabic (GA) and hydroxypropylmethyl cellulose (HPMC) solutions in 25 mM citrate-carbonate buffer at pH 4.6 (Control) and (B) autocorrelation function and intensity-average mean particle size of GGM, GA and HPMC solutions.

for detail structural information of GA. GA is known to form compact globular structure, with molecular aggregates (Sanchez et al., 2018) which explains its smallest mean particle size amongst three hydrocolloids (Fig. 1B). HPMC is a cellulose-derived, semi-synthetic, branched hydrocolloid, similar to GGM (which is substituted by galactose and acetyl units), whose molar mass chosen for this study was similar to that of GGM— ~10 kDa. HPMC is known to have high solubility, due to either methyl or propyl or both groups as backbone substituents. This explains the high transmission through its solution, and the large particle size possibly indicates its solvated polysaccharide chain in solution.

Despite the similarities of GGM with GA in terms of viscosity and with HPMC in terms of molar mass, the low transmission and large particle size of GGM solution suggested the presence of molecular assemblies, which is not typical for an intermediate-molar-mass polysaccharide. The self-association and aggregation behavior in GA have been attributed to its complex chemical composition (Sanchez et al., 2018). Hence, the presence of phenolic compounds and extractives, even in trace amount, could be the origin of GGM assemblies, however this hypothesis needs to be studied separately.

3.2. Effect of solution conditions on GGM assemblies

3.2.1. Effect of pH

Following the previous observation, to understand the solubility of GGM in a wider range of conditions, we studied the effect of the extrinsic factors— solution pH, ionic strength, and the application of high-intensity mechanical shearing (analogous to process conditions applied during emulsion formation). These conditions are relevant to predict the behavior of GGM during product formulation for wide applications. Transmission through the solutions at different solution conditions was measured and the results were also validated by measuring the PSD of the solutions.

The transmission % increased with increasing pH (Fig. 2) which suggested an increased solubility/decrease in particle size of GGM as the solutions went from acidic to alkaline. This can be explained by the well-known fact that most polysaccharides' solubility is enhanced at alkaline pH as the dissolution is promoted by breaking of hydrogen bonds (Guo et al., 2017). The PSD of GGM solutions was polymodal at all pH values (see e.g. Fig. D1, supplementary data). The peaks were in the range of 70–250 nm and 300–2000 nm with a peak maxima around 150 and 700 nm, respectively. A half-peak around 5000 nm was present in the PSD of all studied solutions, including GA and HPMC. This peak was not integrated for the calculation of mean particle size. This peak could be a systematic artefact as they appeared even after sample filtration. The mean particle size of unfiltered GGM solutions did not change significantly with pH ($p = 0.38$). GGM solutions exhibited high size dispersity, which increased the challenge to obtain statistical significance from unfiltered solutions. Although filtration of solutions may bias the results by retaining the large-size particles, to gain some insights on the effect of pH, mean particle size was also compared after the solutions were filtered through 0.7 μm filter. The filtered solutions also showed no statistical significance, however p-value was close to 0.05 ($p = 0.09$). The post-hoc test suggested the probability of increase in particle size with pH. This would happen if there are morphological differences in the aggregates with pH and the large particles in acidic GGM solutions were retained during filtration. Hence, optical microscopy was performed to observe the aggregates (presented further).

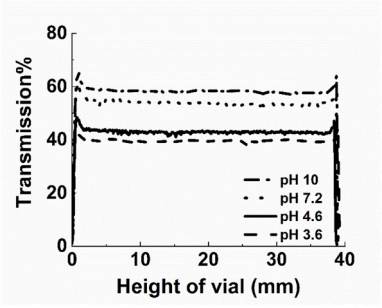

Fig. 2. Transmission (%) of 2% GGM solution on the preparation day at different pH values in 25 mM citrate-carbonate buffer.

3.2.2. Effect of high-intensity mechanical treatment

Next, to understand if mechanical treatment changed the solution properties, we chose to study GGM solution under acidic and alkaline conditions; pH 4.6 and pH 10. Mild acidic pH is common in food products, although alkaline condition is relevant mostly in non-food applications, such as skin-care products. In this study, the aim was to understand the behavior of GGM after mechanical treatment in a wide range of pH.

The transmission of GGM solutions increased after the solutions underwent high-intensity mechanical shearing using Ultraturrax followed by high-pressure homogenization (Fig. 3A). The increased transmission results suggested the enhanced solubility/decrease in particle size of GGM after the high-intensity mechanical shearing, which was also supported by the significant reduction in the mean particle size (Fig. 3B) and change in PSD (Fig. D1, supplementary data). The increase in the transmission of the solutions after the treatment was higher at pH 4.6 than pH 10. This implied the significant change in colloidal state of GGM after the treatment at both pH values and the effect being pronounced at acidic pH.

The TEM images at pH 4.6 showed large loose aggregates of GGM of submicron size (Fig. 3C). Since visualization in TEM is contrast-based, it is essential to mention here that most likely aggregates with high contrast were observed here. The aggregates were observed as sparsely scattered with dense and loose region. Similar observations of xylan aggregates under TEM were reported previously by Westbye et al. (2007). The authors have mentioned different aggregation kinetics for the formation of dense and loose region, which will be discussed further. It is possible that the dense region act as "growth site" to form a loose structural network. In addition, objects resembling nanofibrils were observed. The fibrils' length varied between 3 and 5 nm and some were stacked upon each other. These fibrils in micron range have been designated as fines previously (Kishani et al., 2018). In agreement with the previous study, these fines could adsorb onto GGM and act as nucleation site promoting association, as the surface area for growth increases. Interestingly, methyl cellulose and HPMC have shown fibrillar aggregates at elevated temperature (Bodvik et al., 2010). After high-intensity mechanical shearing, the GGM solution showed a significantly lower number of aggregates (Fig. 3D). When present, only the dense region of the aggregates was observed, and the objects resembling nanofibrils were absent. Digital images from the solutions in Fig. E1 also showed the absence of visible macroscopic aggregates after the treatment.

3.2.3. Effect of ionic strength

To confirm whether electrostatic effects are responsible for the observed GGM assemblies, first the GGM solution was studied after the addition of monovalent cation and second, surface charge density of GGM and zeta potential of the GGM solutions were measured.

Addition of 50 and 100 mM NaCl to the solutions at pH 4.6 and 10 made no significant difference in the transmission % (data not shown), which indicated the negligible presence/absence of charged groups in GGM. The addition of salt to the GGM solution did not change the mean particle size of unfiltered solutions at both acidic pH ($p = 0.23$) and alkaline pH ($p = 0.6$). Their PSD was also polymodal (data not shown), exhibited by heterogeneity at both pH values. The filtered solutions did not show any significant difference in particle size upon the addition of salt at pH 4.6 ($p = 0.28$), however, at pH 10, particle size was higher after the addition of 50 mM NaCl compared to 100 mM NaCl and no salt addition. This indicated addition of small amount of salt might affect the

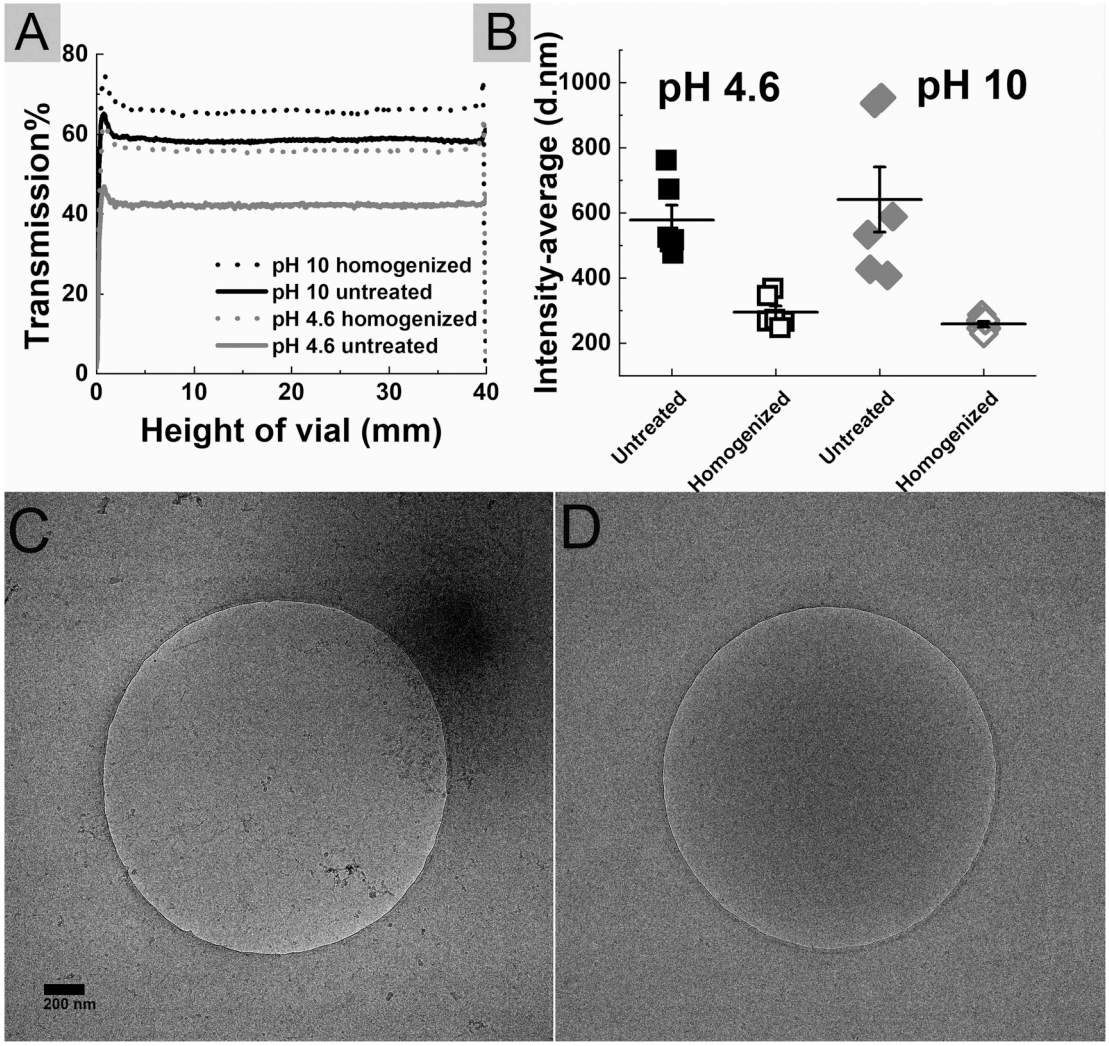

Fig. 3. (A) Transmission % and (B) intensity-average particle size of 2% GGM and at pH 4.6 and 10 before (untreated) and after high-intensity mechanical shearing (homogenized) measured on the preparation day. Horizontal line and vertical whiskers in panel B indicate mean and standard error of mean, respectively. Cryo-TEM images of 2% GGM solution at pH 4.6 on the preparation day (C) before and (D) after high-intensity mechanical shearing. The scale bar in panel A is 200 nm and both images are at the same magnification. Image in panel C was processed to highlight the aggregate. The round objects inside the images originate from sample holder.

solubility at alkaline pH.

From conductometric titration, the surface charge density was 0.24 ± 0.03 mmol/g GGM, which suggested GGM have a very small amount of charged groups. Galactoglucomannans are neutral polysaccharides, hence, based on the carbohydrate, phenolic and extractives analyses of GGM used in our current study, uronic acids and co-extracted phenolic compounds and extractives were most likely the origin of the surface charge. Based on the pH titration curve, the pKa of GGM was 3.85 ± 0.25, which is close to the reported pKa of D-galacturonic acid (3.51) and, methyl derivative of D-glucuronic acid (3.03) (Kohn & Kovac, 1978), and some dioic acids (Moreno & Peinado, 2012; ToolBox, 2017). The ζ-potential of GGM solutions at all studied conditions was less than −15mV (Table 1). The ζ-potential decreased with pH, which suggested the deprotonation of charged groups in GGM above the measured pKa, enhancing electrostatic repulsion between polymer chains, and possibly reducing the association in alkaline conditions. This partly explained the transmission results of GGM solutions at different pH values in Fig. 2, however the overall zeta-potential could not be considered low enough to overcome attractive interaction above pKa (Bhattacharjee, 2016). The pKa of most phenolic compounds are >8 (ToolBox, 2017), hence they would still be protonated even at alkaline pH, if they are linked to GGM in some form. This supported the presence of aggregates at alkaline pH, as indicated by the transmission and PSD results from Fig. 3A and B, respectively.

Table 1
ζ-Potential of GGM solutions measured on the preparation day. Presented values are mean and standard error of mean.

Samples	ζ-potential (mV)
pH 3.6	−3.73 ± 0.35
pH 4.6	−5.90 ± 0.46
pH 4.6100 mM NaCl	−5.14 ± 0.20
pH 4.6 homogenized	−5.26 ± 0.22
pH 7.2	−12.30 ± 0.5
pH 10	−13.85 ± 0.22
pH 10 100 mM NaCl	−8.42 ± 0.22
pH 10 homogenized	−11.20 ± 0.30

To conclude, the present results indicated that the aqueous GGM solutions remained in an aggregated state in both acidic and alkaline pH. The aggregates were disrupted to a large extent after high-intensity mechanical shearing. However, the treatment did not seem to disrupt the assemblies at a molecular level, which suggested the existence of strong interactions in GGM-rich extracts. Poor dissolution of wood hemicelluloses in water has been reported previously. These studies

were about aggregation of GGM and xylans with relatively high molar mass than presently used GGM (Kishani et al., 2018, 2019). Hence, the observed features of PHWE GGM were unique for with an intermediate-molar-mass polysaccharides, which are expected to have high solubility. The low surface charge and zeta potential of GGM suggested that more than macromolecular characteristics, the chemical composition seems to play significant role in the solubility aspect. The co-extracted aromatic residues in GGM, if covalently linked to the polysaccharide structure, could form complexes preventing molecular dissolution, as suggested (Westbye et al., 2007). However, this hypothesis must be studied separately for e.g. by applying targeted enzymatic modification to elucidate detail chemical structure. Ionic strength did not seem to play a significant role, which was expected due to low surface charge in GGM. It was also suspected that the morphology of the aggregates varies with pH, hence optical microscopy was performed on these aggregates (presented further).

3.3. Time dependent self-association of GGM in aqueous solution

PHWE GGM with an intermediate molar mass between that of most hydrocolloids and small-molecular-weight surfactants, was functional to create oil-in-water emulsions with droplet size in sub-micron range. A previous study hypothesized that GGM assemblies at the interface, or in the continuous phase, influences the long-term stability of emulsions (Bhattarai et al., 2019) through time-dependent self-association.

The present data with Turbiscan, PSD and TEM indicated that GGM indeed formed assemblies in solutions at all pH values. Thus, our next step was to study whether these assemblies were more pronounced overtime, i.e. to characterize the time-dependent colloidal stability of GGM solutions. This was studied by monitoring the sedimentation kinetics, mean particle size of GGM solutions stored at RT over 1–4 weeks and optical microscopy imaging. We studied if the extrinsic solution conditions like pH, ionic strength and high-intensity mechanical shearing influenced time-dependent association of GGM solutions.

We compared the time-dependent sedimentation behavior of GGM solutions with GA and HPMC (Fig. 4A). The sedimentation kinetics was evaluated based on Turbiscan Stability Index (TSI) of 0.5% HPMC with 1% GGM and GA solutions as at these concentrations, all the three solutions had a comparable viscosity (Fig. C2, supplementary data).

The TSI indicated that GGM had a faster sedimentation rate followed by GA and HPMC (Fig. 4A), which was supported by the lower light transmission and a higher particle size of GGM observed in Fig. 1A and B. Stoke's law defines that at a similar viscosity, the sedimentation velocity depends on the particle size. However, comparing the particle size and sedimentation behavior of GGM and HPMC, they did not follow Stoke's law. This implies, once again, that GGM formed colloidal solutions with large sedimenting particles compared to GA and HPMC.

In TSI, two regions could be differentiated (Fig. 4B). Phase I, when rapid sedimentation of existing large particles and initiation of association could occur, exhibited by sharp increase in TSI within the first few days of storage. Phase I was pronounced in GGM, followed by GA and HPMC, which was expected due to hypothesized colloidal nature of GGM solutions and presence of molecular aggregates in GA, in contrast to fully dissolved molecules in HPMC solutions. Phase I was followed by Phase II, when the slope of TSI decreased. During Phase II, the slope of TSI decreased in all three hydrocolloid solutions, however in GGM solution, the decrease in the slope was lower i.e. TSI continued to increase. This indicated continuous sedimentation of particles in GGM solutions during storage, which possibly arise from on-going association. We hypothesized three nature of associations for simplicity although in reality several derivations are possible making it a complex association phenomenon; (i) primary cluster particle, when two individual molecules approach to form a cluster (ii) cluster-particle, when the primary cluster approaches an individual molecule to form cluster-particle association and (iii) cluster-cluster, when the cluster approaches another cluster for form a large cluster. Based on TSI profile, it was hypothesized that, compared to GA and HPMC, the system is dynamic in GGM solution; thus, the association continued during storage.

To complement the sedimentation kinetics result, the GGM solutions were also studied for change in the mean particle size during storage in the filtered solutions. It was expected that upon time-dependent association, the change in the mean particle size during storage would be dependent on the kinetics of association and particle size and shape. This indirect approach of depicting time-dependent association was used because, when particle size approaches the upper size range in Dynamic light scattering, other phenomena take place, like sedimentation, thermal currents and number fluctuations, which means that the scattered light intensity will no longer describe purely diffusive motion. Optical microscopy imaging was performed to support the physical analyses.

3.3.1. Effect of pH

First, the GGM solutions at pH 3.6, 4.6, 7.2 and 10 were analyzed for their sedimentation kinetics with TSI (Fig. 5A). The solutions were monitored for 4 weeks, except for pH 10, where the measurement was performed for one week. The anti-microbial capacity of sodium azide is low at alkaline pH, hence the solution at pH 10 showed growth of microbes after a week.

There was a positive relationship between the TSI with pH, similar to the transmission result in Fig. 2A. After the initial rapid increase of TSI, explainable by Phase I hypothesis, the slope of TSI lowered after about 2 days of storage as the solution pH increased, which indicated slower association kinetics. The observed sedimentation behavior could also arise from the differences in the morphology/density of the aggregates. Hence, optical microscopy was performed on these solutions (presented

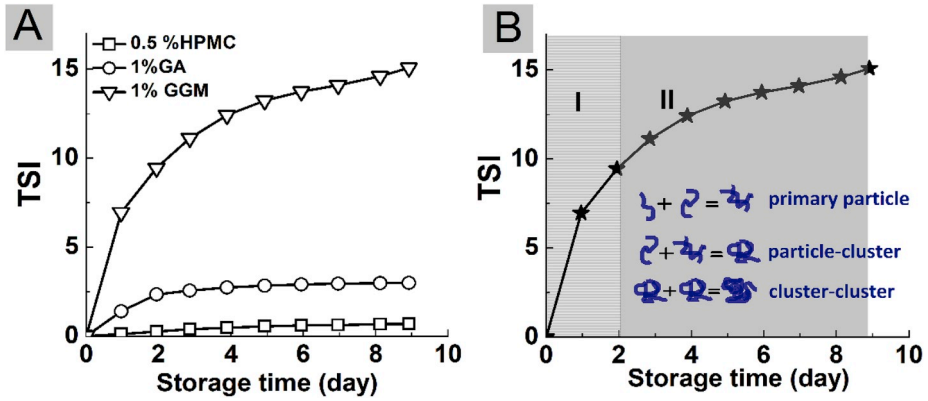

Fig. 4. (A) Turbiscan stability index (TSI) of 0.5% HPMC, and 1% GGM and GA solutions stored for 1 week at RT and (B). hypothesized association phenomenon from TSI profile In figure B, letter I represents Phase I, where rapid sedimentation of large particles + association is hypothesized and letter II represents Phase II where association of different nature is hypothesized.

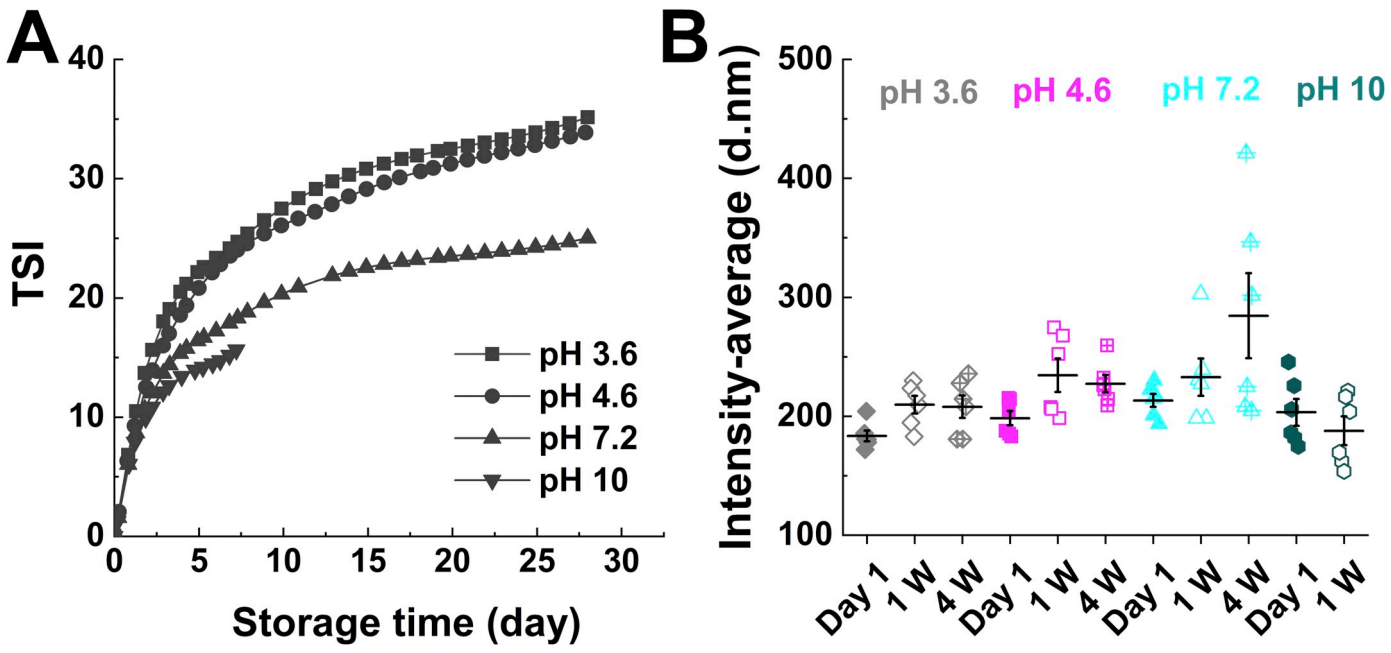

Fig. 5. (A) TSI of 2% GGM solutions measured at different pH values for 1–4 weeks at RT (B) PSD of 2% GGM solutions at pH 3.5, 4.6, 7.2 and 10 measured on the preparation day, 1 week (1W) and after 4 weeks (4W) of storage. All measurements were performed after filtration of samples with 0.7 μm GMF filter. Horizontal line and vertical whiskers indicate mean and standard error of mean, respectively.

further).

Fig. 5B compares the mean particle size of GGM solution measured at different time intervals at acidic, neutral and alkaline pH. Taking mean particle size measured on the preparation day as the reference, at acidic pH, the mean particle size increased after one week of storage; pH 3.6 ($p = 0.01$) and pH 4.6 ($p = 0.03$). At the neutral pH (7.2) and alkaline pH (10), the mean particle size did not change during storage. At pH 7.2, there was no significant change in mean particle size between Day 1 and first week ($p = 0.27$) and between Day 1 and fourth week ($p = 0.08$). Similar result was obtained at pH 10 ($p = 0.37$). Experiments were repeated at pH 4.6 and pH 10, and the results showed the same trend.

GGM solutions were highly size disperse and heterogeneous. The half peak around 5000 nm in PSD (see e.g. Fig. D1) was not included for the calculation of mean particle size, however, we observed the increasing occurrence and intensity area of that peak, which possibly suggests the presence of some large or irregular-shaped particles, and it was more prominent in neutral and alkaline pH.

Optical microscopy imaging was performed on these solutions at three time points over a period of 48 h (Fig. 6).

Two observations were noted from the microscopic images: first, decreased size of aggregates with increasing pH and second, difference in the nature of the aggregates. In acidic pH values, the aggregates seemed to form faster and the observed macroscopic aggregates appeared uniformly denser compared to those in neutral or alkaline pH (Panel C and F vs I and L). The kinetics and the dense morphology of aggregates explain the sedimentation kinetics result in Fig. 5A and complement the TEM images in Fig. 3C. Loose aggregates have more probability to pass through the filter compared to the dense aggregates and could appear as the half peak around 5000 nm as mentioned earlier in PSD. The dense regions at pH 7.2 and 10 appeared as dark spots unevenly spread in the aggregates. These dark spots could originate from the complexation of aggregates. In a previous study, similar dark spots observed together with fibrilar hemicellulose and spherical lignin particles was reported as "lignin-saccharide complex" (Košíková & Joniak, 1978). A very recent study presented evidence of lignin-carbohydrate bonds in crude extract of PHWE GGM (Lahtinen et al., 2019). Although the studied GGM was purified largely by ethanol precipitation, lignin-carbohydrate complexes may exist, and be responsible for the observed self-association. However, this hypothesis has to be studied separately.

In terms of aggregation kinetics, diffusion-limited (DLA) and reaction-limited (RLA) aggregation and their crossover behavior, according to the authors, possibly explains the universal colloid aggregation (Lin et al., 1989). DLA dominates in case of negligible repulsive forces between colloidal clusters, so the probability of them sticking together via Brownian motion defines its kinetics. When the repulsive force between clusters exists but not in sufficient amount, the probability of bond formation between clusters upon their collision defines the kinetics, known as RLA (Lin et al., 1989). DLA is considered rapid producing loose fractal aggregates than RLA. The aggregation phenomenon in acidic region can be attributed to the DLA phenomenon due to low ζ-potential of the GGM solutions and it possibly makes a shift towards RLA with increasing pH, slowing down the kinetics, however the ζ-potential in our tested solution conditions was not high enough to induce sufficient repulsion between clusters. The aggregation could be physical adsorption of one cluster onto another in the initial stage and may develop strong interaction in the later stage due to reorganization.

The time-dependent self-association phenomenon of hydrocolloids is of crucial importance to predict the storage stability of products derived from them. Rye-bran arabinoxylan developed insoluble macroscopic aggregates after three years of storage (Ebringerova, Hromadkova, Burchard, Dolega, & Vorwerg, 1994). In our previous work on GGM-stabilized emulsions, we observed slowing down of the droplet coalescence during storage, particularly after 1 week (Bhattarai et al., 2019). Similarly, flocculation was also observed, which may have occurred due to time-dependent self-association of GGM.

The TSI, PSD, and microscopy images indicated that the pH had a significant role in the self-association behavior of GGM. The nature of aggregates that were formed overtime were not the same at all pH values, which might also explain the differences in the sedimentation behavior, in addition to the faster association kinetics in acidic pH regime.

3.3.2. *Effect of ionic strength*

The results presented in section 3.2.3 failed to show significant role of ionic strength on the solubility properties of GGM. However, we were

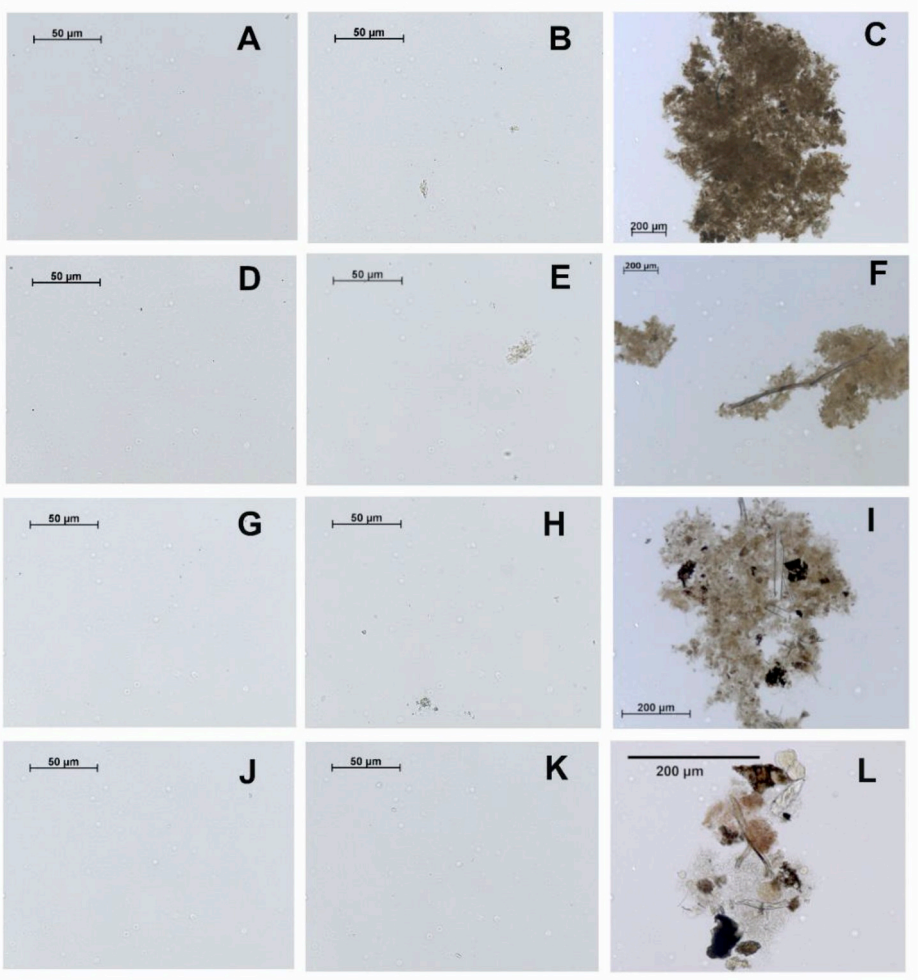

Fig. 6. Optical microscopic images of 2% GGM solutions at pH 3.6 (A, B, C), 4.6 (D, E, F), 7.2 (G, H, I) and 10 (J,K,L). From left to right, each row represents an image taken after approximately 1, 4 and 48 h of storage at RT. Images were processed for better contrast. Scale bar- 50 μm in first two columns on left and 200 μm in the last column on right.

interested to see if their addition affects the time-dependent association behavior of GGM.

Based on TSI, there was no difference in the sedimentation kinetics of the solutions at pH 4.6 upon the addition of NaCl at 50 and 100 mM (Fig. 7). However, at pH 10, it appeared that 100 mM NaCl slowed down the TSI compared to the solution without any salt or with 50 mM NaCl. This can be explained by the salting in effect, when intermolecular attraction between polysaccharides is reduced at low salt concentration.

Based on the PSD, at pH 4.6, the addition of salt failed to significantly

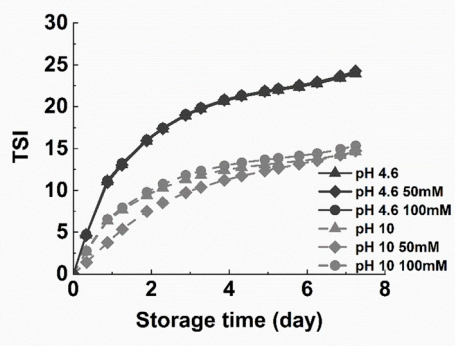

Fig. 7. TSI of 2% GGM solution with and without the addition of 50 mM and 100 mM NaCl at pH 4.6 and pH 10 measured for 1 week.

change the mean particle size of the GGM solution after a week of storage; 50 mM NaCl ($p = 0.17$) and 100 mM NaCl ($p = 0.09$). At pH 10, upon the addition of 50 mM NaCl, the mean particle size did not change after a week of storage ($p = 0.27$), however with 100 mM NaCl, the mean particle size was larger after 1 week of storage ($p = 0.02$) (data not shown). At higher salt concentration, it is possible that dissolution was promoted. The experiment was repeated again for both pH values. This time, we found that there was no significant change in mean particle size upon salt addition at both pH values. Thus, at pH 10, the effect of salting in effect on time-dependent self-association could be minimal, as GGM lack significant surface charge.

Based on the sedimentation behavior and PSD of the solutions, it was concluded that the addition of monovalent cations had a minimal effect on the time-dependent association behavior of GGM in alkaline pH, only at a higher concentration. Resistance to ionic strength offers advantages in a real product matrix, which is constituted of several components. In this regard, polysaccharides-based formulations are also considered superior to protein-based (Dickinson, 2003).

3.3.3. *Effect of high-intensity mechanical shearing*

Results in section 3.2.2 indicated the disruption of the GGM assemblies to a large extent upon high-intensity mechanical shearing. Here, the aim was to study if the disrupted aggregates re-associated during storage. Understanding of this phenomenon is of practical relevance to the stability of products that undergo high-intensity shearing, like

emulsions.

At both pH 4.6 and 10, there were differences in the TSI of GGM solutions before and the high-intensity mechanical shearing (Fig. 8A). However, the difference in TSI was pronounced at pH 4.6, supporting the transmission result in Fig. 3A.

From PSD measurement, the mean particle size of GGM solution at pH 4.6 increased after 1 week of storage ($p = 0.049$), except that in the repeated experiment (data not shown), the increase was significant only after 4 weeks of storage. However, at pH 10, the mean particle size unchanged after 1 week of storage ($p = 0.28$). Optical micrographs of these solutions showed re-association behavior at both pH values, however association appeared rapid at pH 4.6 (Fig. 8 B and C) compared to pH 10 (Fig. 8 D and E).

Hence, it can be concluded that GGM solutions at both pH values showed time-dependent association after destructuration by high-shear mechanical treatment, however, as observed earlier, due to dependence of aggregation kinetics on pH, re-association seemed slower at alkaline pH.

3.4. Considerations on the mechanism of GGM association

Molecular aggregation of hemicelluloses is not an entirely new subject matter (Blake & Richards, 1971; Ebringerova et al., 1994; Ebringerová, Hromádková, & Heinze, 2005). Aggregation of xylans from various plant sources, e.g. glucuronoxylans and arabinoxylans has been understood due to a low number of substituents in their backbone resulting in strong intermolecular bonding. PHWE GGM used in our study had a variety of monosaccharides other than mannose, glucose and galactose, which are the primary constituents of GGM. The considerable amount of xylose units in our GGM extract most likely originates from glucuronoxylan or arabinoglucuronoxylan that are naturally present in minor quantities in softwood. As much as 10% xylose units have been reported in other studies, where GGM were extracted by hot water (Leppänen et al., 2011; Song, Pranovich, & Holmbom, 2013). GGM are considered more soluble than xylans, due to the presence of heterogeneous backbone with mannose and glucose units, and substitution with galactose and acetyl units. Within the GGM family, substitution with a high and low amount of galactose are present. The latter is referred as glucomannans (Sjöström, 1993). Hence, variation in galactose substitution can also affect the solubility. This fact is also supported by Kishani et al. (2018), who studied the molecular solubility of GGM obtained with different extraction and pretreatment method. Although they studied four types of GGM with a wide range of molar mass, which was higher than GGM in our present study, the study indicated higher degree of substitution in GGM improved their molecular solubility. Uronic acids are also known to induce intramolecular hydrogen bonding (Kohn & Kovac, 1978). Dissolution of pectic compounds most likely, galacturonan, rhamnogalacturnoan occurrs when GGM were extracted at high temperatures (Willför, Sjöholm, et al., 2003). The presence of galacturonic acid and rhamnose units in our GGM extract supports the presence of pectic compounds in minor amounts. Hence, the observed aggregates of GGM extracts in our study could partly originate from polysaccharides other than GGM.

Naturally present acetyl groups improve the solubility of hemicelluloses by preventing close packing of polymeric chains. DA can range from 0.3 to 0.4 in native softwood and the DA of GGM in TMP water was reported to be 0.28–0.37 (Hannuksela & Hervé du Penhoat, 2004). Both high and low DA can reduce solubility of hemicelluloses, as demonstrated previously in xylans (Gröndahl, Teleman, & Gatenholm, 2003). The DA of GGM in our study was 0.32, which is slightly higher than reported by Kishani et al. (Kishani et al., 2018). The acetyl groups are sensitive to alkaline pH; hence, the observed solution behavior at alkaline pH could partly originate due to alkaline deacetylation leading to decreased solubility.

Presence of non-polysaccharide residues, like proteins and lignin, have also been linked to the polysaccharide aggregation (Ebringerová et al., 2005). Hence, the interactions of residual phenolic compounds in GGM may partially, but not alone be responsible for the observed association phenomenon in GGM.

4. Conclusion

The solubility of hydrocolloids and the effect of extrinsic solution conditions are essential aspects to consider when designing and predicting their behavior in a complex multiphasic system. For the first time, the present study exhibited the colloidal nature of aqueous solutions of PHWE GGM formed from their assemblies. Compared to GA and HPMC, GGM exhibited features of a complex colloidal system. In contrast to what is expected from an intermediate molar mass polysaccharide like GGM, partial molecular dispersion and time-dependent self-association of GGM was observed at all pH values. A large number of molecular assemblies could not be destructured by applying high-intensity mechanical shearing force, which indicated the existence of strong interactions. The time-dependent self-association possibly originates from weak forces like hydrogen-bonding and physical entanglements, driven by diffusion. The self-association and their kinetics during storage were more pronounced in acidic pH than in alkaline. The low surface charge and dissociation constant do not fully explain the self-

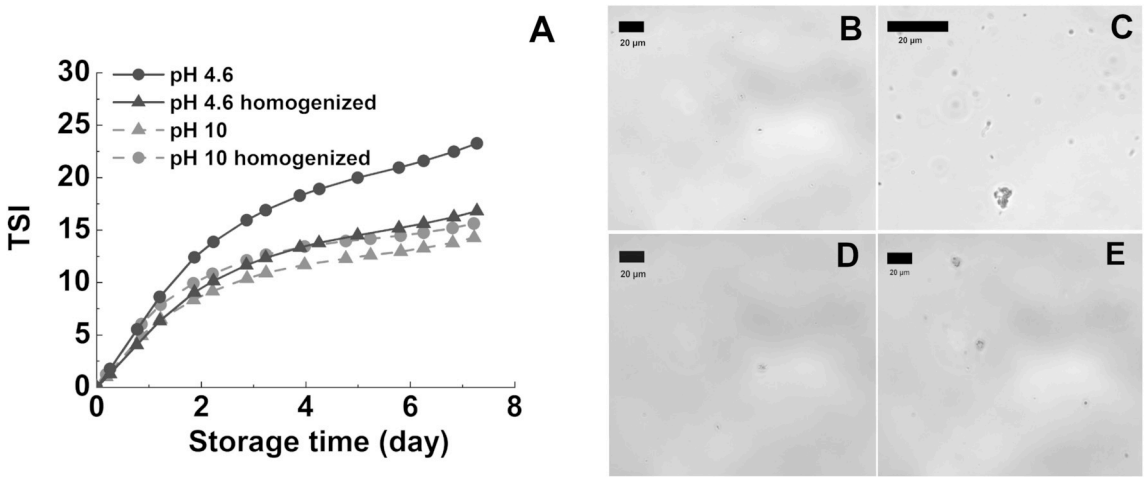

Fig. 8. (A) TSI of 2% GGM solutions before and after high-intensity mechanical shearing (homogenized) at pH 4.6 and 10 measured for 1 week. Optical microscopic images of 2% GGM solutions at (B, C) pH 4.6 and (D, E) pH 10. Each row from left to right represent images after 1 h of preparation and 48 h of storage at RT. Images were converted to greyscale and processed for better contrast. Scale bar = 20 μm.

association phenomenon, which also explains the non-negligible effect of monovalent cation on GGM.

The self-association behavior of GGM and its time-dependency suggest that the system is dynamic, which potentially have an important role in the stabilization of dispersions formed by GGM. This type of "partial solubility" characteristic of polysaccharides can impart the complex stabilization mechanism of the multiphasic systems and can be desirable as opposed to full dissolution of hydrocolloids. The unique colloidal features of GGM can be utilized to design functional nano/microstructures alone or in combination with other components. In this regard, GGM obtained from biomass resource has high potential in the development of complex, functional food products.

Declaration of competing interest

There are no conflicts of interest to declare.

CRediT authorship contribution statement

Mamata Bhattarai: Conceptualization, Methodology, Investigation, Formal analysis, Visualization, Writing - original draft. **Fabio Valoppi:** Methodology, Formal analysis, Writing - review & editing. **Sami-Pekka Hirvonen:** Investigation, Writing - review & editing. **Sami Hietala:** Investigation, Writing - review & editing. **Petri Kilpeläinen:** Writing - review & editing, Investigation. **Vladimir Aseyev:** Methodology, Validation, Writing - review & editing. **Kirsi S. Mikkonen:** Conceptualization, Supervision, Writing - review & editing.

Acknowledgements

The Doctoral Program of Food Chain and Health (University of Helsinki) and Academy of Finland (grant no 305517) are acknowledged for funding MB and FV, respectively. Dr. Maarit Lahtinen is acknowledged for a fruitful discussion on aggregation behavior results. We thank Benita Löflund, and Pasi Laurinmäki, University of Helsinki for technical assistance in performing Cryo-TEM imaging, which was carried out with support of the Biocenter Finland and Instruct-FI CryoEM core facility, University of Helsinki. Julia Varis is greatly acknowledged for drawing the graphical abstract. The authors also acknowledge Miia Collander from University of Helsinki for her assistance in performing conductometric titration experiment.

Appendix A. Supplementary data

Supplementary data related to this article can be found at https://doi.org/10.1016/j.foodhyd.2019.105607.

References

Bhattacharjee, S. (2016). DLS and zeta potential – what they are and what they are not? *Journal of Controlled Release, 235*, 337–351. https://doi.org/10.1016/j.jconrel.2016.06.017.

Bhattarai, M., Pitkanen, L., Kitunen, V., Korpinen, R., Ilvesniemi, H., Kilpelainen, P. O., … Mikkonen, K. S. (2019). Functionality of spruce galactoglucomannans in oil-in-water emulsions. *Food Hydrocolloids, 86*, 154–161. https://doi.org/10.1016/j.foodhyd.2018.03.020.

Blake, J. D., & Richards, G. N. (1971). Evidence for molecular aggregation in hemicelluloses. *Carbohydrate Research, 18*(1), 11–21. https://doi.org/10.1016/S0008-6215(00)80254-2.

Bodvik, R., Dedinaite, A., Karlson, L., Bergström, M., Bäverbäck, P., Pedersen, J. S., … Claesson, P. M. (2010). Aggregation and network formation of aqueous methylcellulose and hydroxypropylmethylcellulose solutions. *Colloids and Surfaces A: Physicochemical and Engineering Aspects, 354*(1), 162–171. https://doi.org/10.1016/j.colsurfa.2009.09.040.

Borkowski, B. M. (2005). Buffer capacity. Retrieved from www.chembuddy.com.

Dickinson, E. (2003). Hydrocolloids at interfaces and the influence on the properties of dispersed systems. *Food Hydrocolloids, 17*(1), 25–39. https://doi.org/10.1016/S0268-005X(01)00120-5.

Dickinson, E. (2017). Biopolymer-based particles as stabilizing agents for emulsions and foams. *Food Hydrocolloids, 68*, 219–231. https://doi.org/10.1016/j.foodhyd.2016.06.024.

Ebringerova, A., Hromadkova, Z., Burchard, W., Dolega, R., & Vorwerg, W. (1994). Solution properties of water-insoluble rye-bran arabinoxylan. *Carbohydrate Polymers, 24*(3), 161–169. https://doi.org/10.1016/0144-8617(94)90126-0.

Ebringerová, A., Hromádková, Z., & Heinze, T. (2005). Hemicellulose. In T. Heinze (Ed.), *Polysaccharides I: Advances in polymer science* (Vol 186, pp. 1–67). Berlin: Springer.

Ministry of Economic Affairs and Employment. (2017). *Wood-based bioeconomy solving global challenges*. www.bioeconomy.fi/publication-wood-based-bioeconomy-solving-global-challenges/. (Accessed 14 August 2017).

Farris, S., Mora, L., Capretti, G., & Piergiovanni, L. (2012). Charge density quantification of polyelectrolyte polysaccharides by conductometric titration: An analytical chemistry experiment. *Journal of Chemical Education, 89*(1), 121–124. https://doi.org/10.1021/ed200261w.

Fishman, M. L., Cooke, P., Hotchkiss, A., & Damert, W. (1993). Progressive dissociation of pectin. *Carbohydrate Research, 248*, 303–316. https://doi.org/10.1016/0008-6215(93)84136-T.

Gittings, M. R., Cipelletti, L., Trappe, V., Weitz, D. A., In, M., & Marques, C. (2000). Structure of guar in solutions of H2O and D2O: an ultra-small-angle light-scattering study. *The Journal of Physical Chemistry B, 104*(18), 4381–4386. https://doi.org/10.1021/jp9943833.

Gröndahl, M., Teleman, A., & Gatenholm, P. (2003). Effect of acetylation on the material properties of glucuronoxylan from aspen wood. *Carbohydrate Polymers, 52*(4), 359–366. https://doi.org/10.1016/S0144-8617(03)00014-6.

Guo, M. Q., Hu, X., Wang, C., & Ai, L. (2017). Polysaccharides: Structure and solubility. In *Solubility of Polysaccharides*. London, United Kingdom: IntechOpen Limited.

Hannuksela, T., & Hervé du Penhoat, C. (2004). NMR structural determination of dissolved O-acetylated galactoglucomannan isolated from spruce thermomechanical pulp. *Carbohydrate Research, 339*(2), 301–312. https://doi.org/10.1016/j.carres.2003.10.025.

Kilpeläinen, P. O., Hautala, S. S., Byman, O. O., Tanner, L. J., Korpinen, R. I., Lillandt, M. K. J., … Ilvesniemi, H. S. (2014). Pressurized hot water flow-through extraction system scale up from the laboratory to the pilot scale. *Green Chemistry, 16*(6), 3186–3194. https://doi.org/10.1039/C4GC00274A.

Kim, S., Hyun, K., Moon, J. Y., Clasen, C., & Ahn, K. H. (2015). Depletion stabilization in nanoparticle–polymer suspensions: Multi-Length-Scale Analysis of microstructure. *Langmuir, 31*(6), 1892–1900. https://doi.org/10.1021/la504578x.

Kishani, S., Escalante, A., Toriz, G., Vilaplana, F., Gatenholm, P., Hansson, P., et al. (2019). Experimental and theoretical evaluation of the solubility/insolubility of spruce xylan (arabino glucuronoxylan). *Biomacromolecules, 20*(3), 1263–1270. https://doi.org/10.1021/acs.biomac.8b01686.

Kishani, S., Vilaplana, F., Xu, W., Xu, C., & Wågberg, L. (2018). Solubility of softwood hemicelluloses. *Biomacromolecules, 19*(4), 1245–1255. https://doi.org/10.1021/acs.biomac.8b00088.

Kohn, R., & Kovac, P. (1978). Dissociation constants of D-galacturonic and D-glucuronic acid and their O-methyl derivatives. *Chemické Zvesti, 32*(4), 478–485.

Košíková, B., Zákutná, L., & Joniak, D. (1978). Investigation of the lignin-saccharidic complex by electron microscopy. *Holzforschung, 32*(1), 15–18. https://doi.org/10.1515/hfsg.1978.32.1.15.

Lahtinen, M. H., Valoppi, F., Juntti, V., Heikkinen, S., Kilpeläinen, P. O., Maina, N. H., & Mikkonen, K. S. (2019). Lignin-Rich PHWE Hemicellulose Extracts Responsible for Extended Emulsion Stabilization. *Frontiers in Chemistry, 7*, 871. https://doi.org/10.3389/fchem.2019.00871.

Lehtonen, M., Merinen, M., Kilpeläinen, P. O., Xu, C., Willför, S., & Mikkonen, K. S. (2018). Phenolic residues in spruce galactoglucomannans improve stabilization of oil-in-water emulsions. *Journal of Colloid and Interface Science, 512*, 536–547. https://doi.org/10.1016/j.jcis.2017.10.097.

Leppänen, K., Spetz, P., Pranovich, A., Hartonen, K., Kitunen, V., & Ilvesniemi, H. (2011). Pressurized hot water extraction of Norway spruce hemicelluloses using a flow-through system. *Wood Science and Technology, 45*(2), 223–236. https://doi.org/10.1007/s00226-010-0320-z.

Lin, M., Lindsay, H. M., Weitz, D., Ball, R., Klein, R., & Meakin, P. (1989). Universality in colloid aggregation. *Nature, 339*(6223), 360. https://doi.org/10.1038/339360a0.

Mikkonen, K. S., Kirjoranta, S., Xu, C., Hemming, J., Pranovich, A., Bhattarai, M., … Willför, S. (2019). Environmentally-compatible alkyd paints stabilized by wood hemicelluloses. *Industrial Crops and Products, 133*, 212–220. https://doi.org/10.1016/j.indcrop.2019.03.017.

Mikkonen, K. S., Merger, D., Kilpeläinen, P., Murtomäki, L., Schmidt, U. S., & Wilhelm, M. (2016). Determination of physical emulsion stabilization mechanisms of wood hemicelluloses via rheological and interfacial characterization. *Soft Matter, 12*(42), 8690–8700. https://doi.org/10.1039/C6SM01557C.

Mikkonen, K. S., Xu, C., Berton-Carabin, C., & Schroën, K. (2016). Spruce galactoglucomannans in rapeseed oil-in-water emulsions: Efficient stabilization performance and structural partitioning. *Food Hydrocolloids, 52*, 615–624. https://doi.org/10.1016/j.foodhyd.2015.08.009.

Moreno, J., & Peinado, R. (2012). Carboxylic acids: Structure and properties. In *Enological chemistry* (pp. 109–120). San Diego: Academic Press.

Nishinari, K., Takemasa, M., Zhang, H., & Takahashi, R. (2007). 2.19 - storage plant polysaccharides: Xyloglucans, galactomannans, glucomannans. In H. Kamerling (Ed.), *Comprehensive glycoscience* (pp. 613–652). Oxford: Elsevier.

Pitkänen, L., Heinonen, M., & Mikkonen, K. S. (2018). Safety considerations of plant polysaccharides for food use: A case study on phenolic-rich softwood galactoglucomannan extract. *Food & Function, 9*(4), 1931–1943. https://doi.org/10.1039/C7FO01425B.

Ratcliffe, I., Williams, P. A., Viebke, C., & Meadows, J. (2005). Physicochemical characterization of konjac glucomannan. *Biomacromolecules, 6*(4), 1977–1986. https://doi.org/10.1021/bm0492226.

Sanchez, C., Nigen, M., Mejia Tamayo, V., Doco, T., Williams, P., Amine, C., et al. (2018). Acacia gum: History of the future. *Food Hydrocolloids, 78*, 140–160. https://doi.org/10.1016/j.foodhyd.2017.04.008.

Schoultz, S. V. (2015). *U.S. Patent No.14,413,409*. Washington, DC: U.S. Patent and Trademark Office.

Semenov, A. N., & Shvets, A. A. (2015). Theory of colloid depletion stabilization by unattached and adsorbed polymers. *Soft Matter, 11*(45), 8863–8878. https://doi.org/10.1039/C5SM01365H.

Sjöström, E. (1993). *Wood chemistry: Fundamentals and applications*. Gulf professional publishing.

Song, T., Pranovich, A., & Holmbom, B. (2013). Separation of polymeric galactoglucomannans from hot-water extract of spruce wood. *Bioresource Technology, 130*, 198–203. https://doi.org/10.1016/j.biortech.2012.11.149.

Tadros, T. F. (2017). *Basic principles of interface science and colloid stability* (Vol. 1). Berlin Boston: De Gruyter.

ToolBox, E. (2017). Phenols, alcohols and carboxylic acids - pKa values. https://www.engineeringtoolbox.com/paraffinic-benzoic-hydroxy-dioic-acids-structure-pka-carboxylic-dissociation-constant-alcohol-phenol-d_1948.html.

Valoppi, F., Lahtinen, M., Bhattarai, M., Kirjoranta, S. J., Juntti, V. K., Peltonen, L., … Mikkonen, K. S. (2019). Centrifugal fractionation of softwood extracts improves biorefinery workflow and yields functional emulsifiers. *Green Chemistry, 21*, 4691–4705. https://doi.org/10.1039/C9GC02007A.

Walter, R. H., & Matias, H. L. (1991). Pectin aggregation number by light scattering and reducing end-group analysis. *Carbohydrate Polymers, 15*(1), 33–40. https://doi.org/10.1016/0144-8617(91)90017-7.

Westbye, P., Köhnke, T., Glasser, W., & Gatenholm, P. (2007). The influence of lignin on the self-assembly behavior of xylan rich fractions from birch *(Betula pendula)*. *Cellulose, 14*, 603–613. https://doi.org/10.1007/s10570-007-9178-0.

Whistler, R. L. (1973). Solubility of polysaccharides and their behavior in solution. In *Carbohydrates in solution* (Vol. 117, pp. 242–255). American Chemical Society.

Willför, S., Rehn, P., Sundberg, A., Sundberg, K., & Holmbom, B. (2003). Recovery of water-soluble acetylgalactoglucomannans from mechanical pulp of spruce. *Tappi Journal, 2*(11), 27–32.

Willför, S., Sjöholm, R., Laine, C., Roslund, M., Hemming, J., & Holmbom, B. (2003). Characterisation of water-soluble galactoglucomannans from Norway spruce wood and thermomechanical pulp. *Carbohydrate Polymers, 52*(2), 175–187. https://doi.org/10.1016/S0144-8617(02)00288-6.

Willför, S., Sundberg, K., Tenkanen, M., & Holmbom, B. (2008). Spruce-derived mannans – a potential raw material for hydrocolloids and novel advanced natural materials. *Carbohydrate Polymers, 72*(2), 197–210. https://doi.org/10.1016/j.carbpol.2007.08.006.

Xu, C., Leppänen, A.-S., Eklund, P., Holmlund, P., Sjöholm, R., Sundberg, K., et al. (2010). Acetylation and characterization of spruce (Picea abies) galactoglucomannans. *Carbohydrate Research, 345*(6), 810–816. https://doi.org/10.1016/j.carres.2010.01.007.

Xu, C., Willför, S., Holmlund, P., & Holmbom, B. (2009). Rheological properties of water-soluble spruce O-acetyl galactoglucomannans. *Carbohydrate Polymers, 75*(3), 498–504. https://doi.org/10.1016/j.carbpol.2008.08.016.